Superalloys 2004
Edited by K.A. Green, T.M. Pollock, H. Harada,
T.E. Howson, R.C. Reed, J.J. Schirra, and S. Walston
TMS (The Minerals, Metals & Materials Society), 2004

Influence of Solidification Conditions on TCP Phase Formation, Casting Porosity and High Temperature Mechanical Properties in a Re-Containing Nickel-Base Superalloy with Columnar Grain Structure

A. Volek, R. F. Singer

University of Erlangen-Nürnberg, Dept. of Materials Science and Engineering, Institute II, Martensstr. 5, D-91058 Erlangen

Keywords: DS-superalloy, segregation, TCP phase formation, porosity, creep, fatigue

Abstract

A coarse and a fine dendrite structure were produced using the newly developed DS-superalloy *ExAl7* (≅ IN792 with 2-3 wt.-% Re) by changing the conditions of directional solidification. The two microstructures differed in their primary dendrite arm spacing by a factor of 1.6. During aging, very fine TCP phase precipitates (length approximately 20 µm, volume fraction ~ 1 %) were precipitated in the dendrite core, where the refractory element content was particularly high due to segregation. The finer dendrite structure resulted in a lesser tendency for TCP phase formation and smaller (but more numerous) casting pores. Creep strength was not affected by the dendrite size, apparently because TCP phase size and amount were still so small. Fatigue strength, however, was much improved by the finer dendrite structure. Casting pores were found to be somewhat larger than the TCP phases under the conditions investigated and to act as crack starters in fatigue.

Introduction

The interest in the development of nickel-base superalloys continues to be very large because any increase in high temperature capability leads to improved gas turbine efficiency [1]. Recently developed alloys contain high amounts of refractory elements, such as W, Mo und Re, which act as solid solution strengtheners at high temperature. The introduction of these elements, however, makes the microstructure more susceptible to the formation of topologically closed packed (TCP) phases during long-term service [2, 3]. Several different types of TCP phases have been observed in the past. Newly developed single crystal and columnar grain nickel-base superalloys containing Re tend to form TCP phase precipitates located within the cores of the dendrite structure due to residual segregation [4]. In earlier work of the present authors evidence was presented that this type of TCP phase (most likely orthorhombic P phase) is not detrimental to creep rupture life [5]. In the present paper experimental results will be reported which complement the earlier evidence. In addition the effect of TCP phase formation on fatigue properties will be considered.

Dendrite arm spacing in superalloy components can be reduced significantly by using the casting technique of Liquid Metal Cooling (LMC) rather than the standard Bridgman process [6-8]. The advantage of LMC is due to higher thermal gradients and solidification rates. The potential to improve mechanical properties by using LMC casting technology will also be discussed here.

Experimental Procedure

Table I*:* Nominal chemical compositions of the investigated alloys IN792 and *ExAl7* [9].

	Cr	Co	Mo	W	Ta	Al	Ti	Re
ExAl7	12.0	9.0	1.8	3.5	4.0	3.4	3.9	2-3
IN792	12.5	9.0	1.9	4.0	4.0	3.5	3.9	-

Rods of 180 mm length with a diameter of 12 mm or 25 mm, respectively, with a columnar grain structure were produced by directional solidification in a laboratory scale investment casting unit. The new developed DS-alloy *ExAl7* [9] and for comparison purposes IN792 in selected instances were used for the investigation (for alloy compositions see **Tab. I**). By varying the casting parameters (see **Tab. II**) two different sets of samples could be obtained, one with a coarse dendrite structure and one with a fine dendrite structure.

Table II: By varying the casting conditions two different kinds of microstructure were produced. λ_I: primary dendrite arm spacing, *Ø*: diameter of the cast rods, ϑ_c: casting temperature, ϑ_m: mould temperature, *v*: withdrawal speed during solidification.

Dendrites	λ_I *(µm)*	*Ø (mm)*	ϑ_c *(°C)*	ϑ_m *(°C)*	*v (mm/min)*
Coarse	290	25	1550	1450	3
Fine	180	12	1550	1500	6

The directionally solidified rods received a solution and homogenisation heat treatment at 1220 °C or 1240 °C for 4 h followed by a precipitation heat treatment at 1080 °C for 4 h and 845 °C for 24 h in air. Metallographic samples were cut perpendicular to the [001] solidification direction. Metallographic preparation included grinding, polishing and chemical etching with so called molybdenum acid. This etchant consists of 100 ml H_20 + 100 ml HNO_3 + 100 ml HCl + 3 g MoO_3 and takes the γ' precipitates into solution ("negative etching").

Optical microscopy with a Zeiss Axiophot microscope connected to an image analysis system ImageC was used for pore size evaluation and determination of primary dendrite arm spacing λ_I.

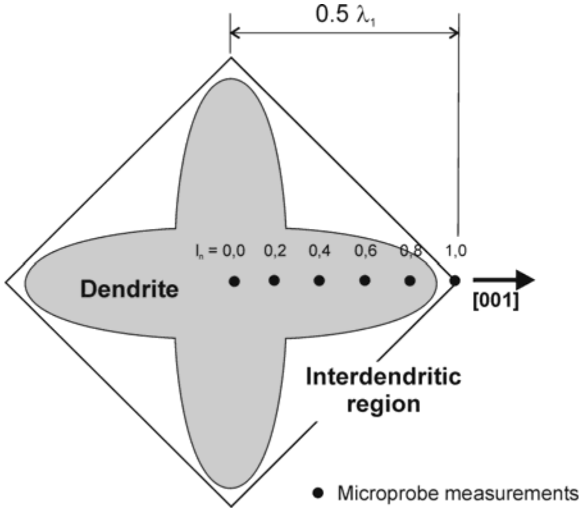

Figure 1: Schematic representation of the dendrite structure in the present alloys. The solidification direction is perpendicular to the plane of the drawing. The growing dendrite is drawn in grey. Microprobe measurements are indicated by black dots. They start at the dendrite core and follow the dendrite arm towards the interdendritic region.

Mechanical samples (creep rupture and fatigue) were cut parallel to the [001] solidification direction according to German standard DIN 50118 for creep rupture testing (Ø 5.3 mm, gage length 25 mm) and Roell Amsler specifications for fatigue testing (Ø 5 mm, gage length 20 mm). Creep rupture tests were performed at constant load at 850 °C in air using ATS 2330 Series Lever Arm Testers. Dynamic tests were performed using a high frequency Röll Amsler Pulser 2 HFP 421 at 800 °C. A stress ratio of R = –1 was selected. The stress amplitude varied between 200 MPa and 400 MPa.

To detect the influence of TCP phase formation some samples were pre-aged at 850 °C for 100 h, 200 h, 300 h, 400 h, 500 h and 700 h in air atmosphere before mechanical testing.

Results

Effect of dendrite structure on TCP phase and porosity formation
As pointed out above, by using different solidification conditions two different kinds of dendrite structure could be produced in the *ExAl7* alloy. **Fig. 2** shows the two structures in the as cast condition. The coarse dendrite structure has an average primary dendrite arm spacing of λ_I = 290 µm, the fine dendrite structure of λ_I = 180 µm.

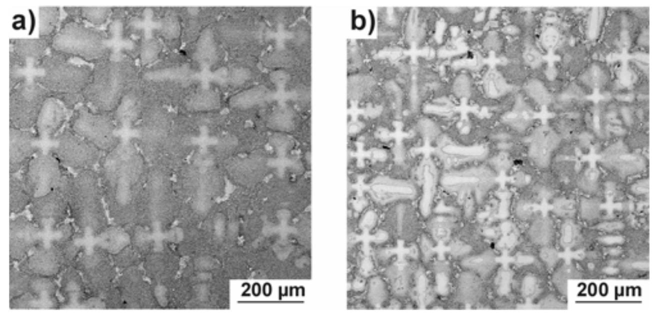

Figure 2: By use of different casting parameters (see **Tab. 2**), two different dendrite structures could be produced in alloy *ExAl7*. Optical micrographs in the as cast condition. a) coarse dendrite structure, $\lambda_1 \approx 290$ µm and b) fine dendrite structure, $\lambda_1 \approx 180$ µm.

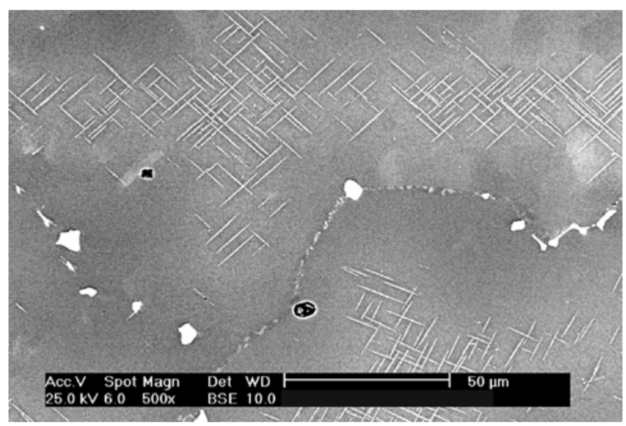

Figure 3: SEM image showing TCP phase formation predominantly within dendrite cores after isothermal aging of alloy *ExAl7* at 850 °C / 500 h. The TCP phase appears as bright needles parallel to the [110]-direction.

After standard heat treatment and additional isothermal aging for 500 h at 850 °C, TCP phase formation occurs as can be seen from **Fig. 3**. TCP phase formation is found localized within dendrite cores only. Microprobe measurements reveal that even after homogenisation heat treatment the alloying elements are not distributed homogeneously along the dendrite arm (**Fig. 4**). Segregation is particularly severe for the elements Re, W, Ti and Ta. Re and W are enriched in the dendrite core while Ti and Ta are enriched in the interdendritic regions.

Very little TCP phase formation can already be observed. During isothermal aging the amount of TCP phase increases with increasing aging time. As **Fig. 5** shows, TCP phase formation is stronger in the samples with coarse dendrite structure. Quantita-

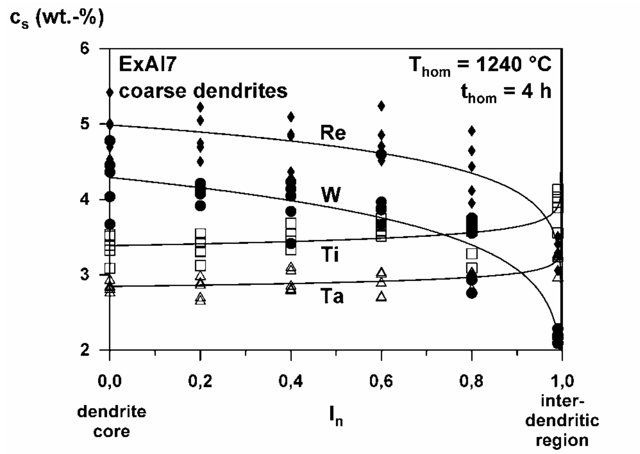

Figure 4: Element concentration c_s as a function of normalized dendrite arm length l_n. Microprobe measurements along the [001] direction of a secondary dendrite arm were performed to show residual segregation after homogenisation heat treatment. l_n corresponds to the relative position of the measurement on the dendrite arm as explained in **Fig. 1**.

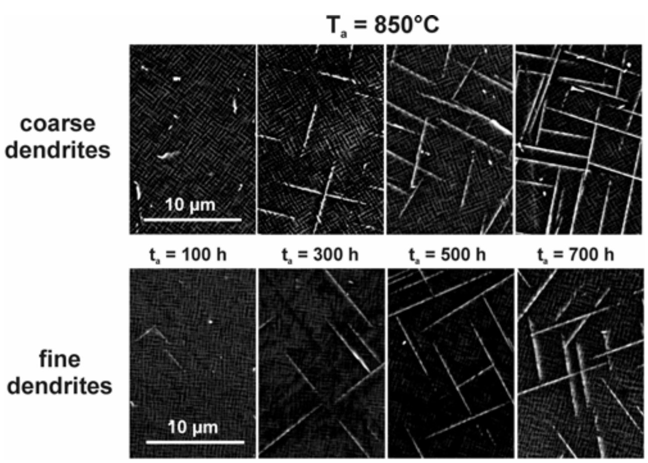

Figure 5: SEM images depicting TCP phase formation in dendrite cores of samples with coarse and fine dendrite structure of alloy *ExAl7* after different isothermal pre-aging times at 850 °C.

Solidification conditions and dendrite structure cause important differences in casting porosity. Analysing the porosity in coarse and fine dendrite structure by optical microscopy, a total pore area fraction of around 0.3 % in both structures was determined. The average pore distance is 240 µm in the coarse dendrite structure and 160 µm in the fine dendrite structure which is in good agreement with the measured primary dendrite arm spacing of both microstructures. A frequency distribution profile of the pore size is shown in **Fig. 7**. It can be seen that the finer structure contains a higher number of pores but with a lower cross sectional area. Maximum pore size detected in the fine structure is around 400 μm^2. Maximum pore size of coarse structure samples is up to 900 μm^2. Assuming a spheroidal shape of the pores this corresponds to a diameter of 22 µm and 34 µm, respectively.

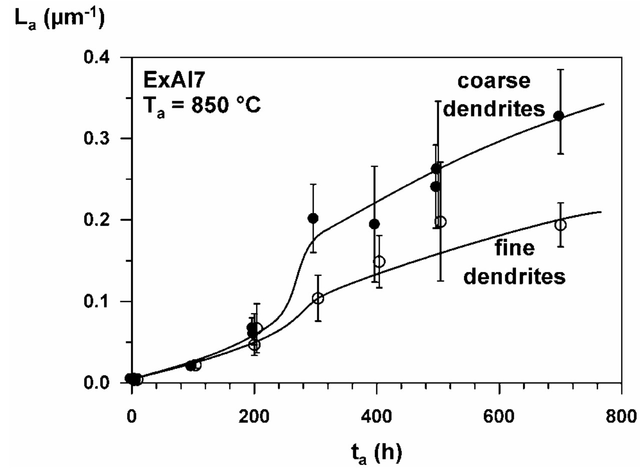

Figure 6: TCP needle area fraction L_a (total length per unit area) as a function of aging time t_a. Dendrite core areas were evaluated in the SEM (see **Fig. 6**). TCP phase formation is stronger in the coarse dendrite structure.

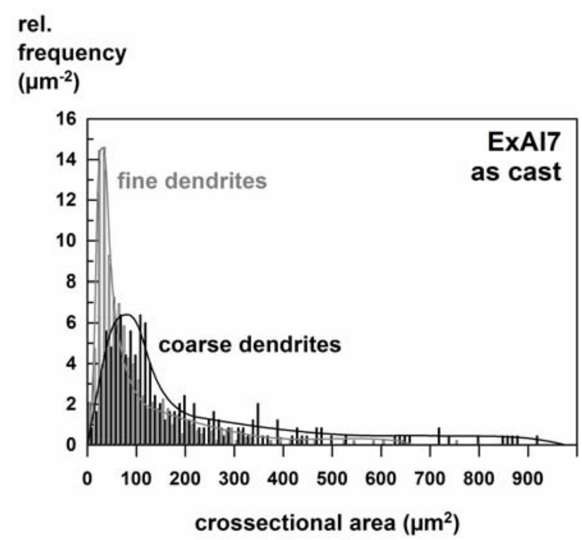

Figure 7: Casting pore size distribution in coarse and fine dendrite structure.

<u>Effect of TCP phase formation on creep</u>

The *ExAl7* alloy described in the previous section with its two microstructures was creep rupture tested at 850 °C and 550 MPa. The results are shown in **Fig. 8**. There is no notable difference in strength, i.e. dendrite size and the ensuing strength of TCP phase formation do not seem to have an effect.

For comparison purposes, rupture data for the alloy IN792 was generated and also included in **Fig. 8**. IN792 is a rather similar alloy as *ExAl7* (**Tab. 2**) but contains no Re and, therefore, does effect of Re is to be expected, as Re is known to be a very effective solid solution strengthener.

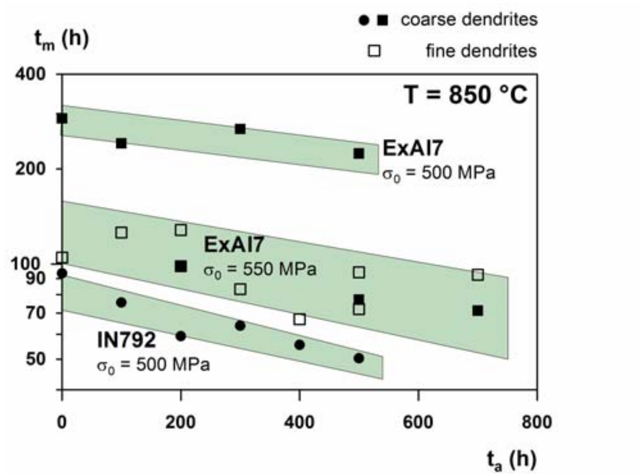

Figure 8: Time to fracture t_m in creep rupture testing as a function of pre-aging time t_a. Re additions improve rupture life (see 500 MPa results). No effect of TCP phase formation is apparent (see 550 MPa results).

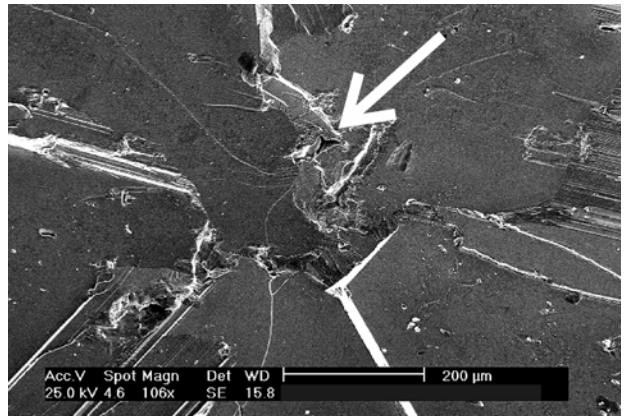

Figure 10: Fracture surface of a HCF specimen of alloy *ExAl7*. The arrow indicates a casting pore which acts as the crack initiation site.

Effect of TCP phase formation and porosity on fatigue

HCF strength of *ExAl7* with the fine dendrite structure is improved compared with the coarse dendrite structure (see **Fig. 9**). Careful examination of the fracture surface reveals that fatigue cracks initiate from casting pores rather than from TCP needles (**Fig. 10**). As such the improvement in fatigue strength must be due to smaller pore size rather than reduced amount of TCP phase formation.

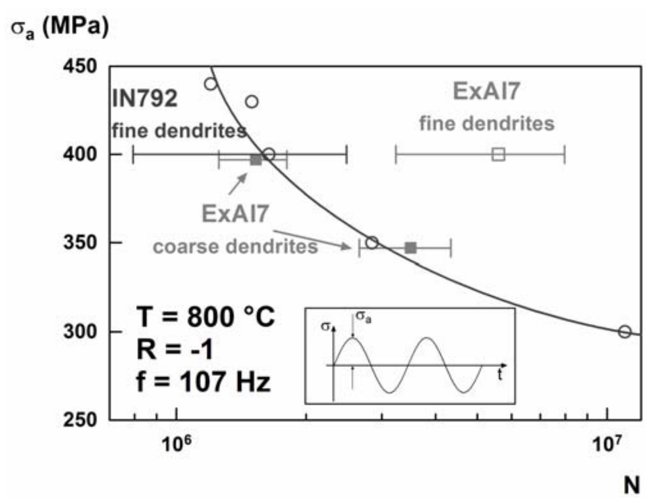

Figure 9: Stress amplitude σ_a as a function of the number of cycles to failure N tested in the standard heat treated condition. Re additions improve fatigue strength. The finer dendrite structure displays better fatigue strength than the coarser structure.

In addition **Fig. 9** allows to compare the HCF strength of *ExAl7* and conventional IN792 in the standard heat treated condition. As in creep, *ExAl7* turns out to be the stronger alloy. The positive

Discussion

Effect of the casting technique on microstructure and properties

The Liquid Metal Cooling (LMC) casting technique is able to produce finer dendrite structures than the conventional Bridgman technique, as has been shown again and again in the literature [6-8]. In the present paper a coarse and a fine microstructure were compared which both in effect were produced in a Bridgman apparatus using different casting conditions, but which were meant to represent the difference between a LMC and a Bridgman turbine blade. With primary dendrite arm spacing of 180 µm and 290 µm we have only been able to produce values that might be typical for the situation in small aero-engine blades. The typical values for large industrial turbine blades may be more like 350 µm in the LMC process and 600 µm in the Bridgman process [6]. As such, our results are more typical for the situation with very small blades.

The finer dendrite structure led to reduced TCP phase formation and also resulted in reduced size of casting pores. The TCP phases under the present conditions were found not to affect the mechanical properties. This could be different in an industrial turbine blade, where dendrite arm spacings will be much coarser with ensuing consequences on microsegregation in the as cast and homogenized state.

Our creep results show that the loss of stress rupture life with pre-aging time occurs in equal measure in the TCP phase free alloy IN792 as well as in the TCP phase prone alloy *ExAl7* (**Fig. 8**). There is also no noticeable difference between the coarse and the fine dendrite structure in spite of the different amount of TCP phase formation. It is assumed, therefore, that the decrease in rupture life is not associated with TCP phase formation, but rather with over-aging of the precipitate structure. The amount of TCP phase formation is obviously still too small to have an effect on creep life. In earlier work we have also shown that small amounts of TCP phase precipitates similar to the present case are not harmful, while stronger amounts are, and explained this by the loss of solution strengthening caused by TCP phase formation [5].

It was observed in the present investigation that TCP phase forms only in the dendrite core (**Fig. 4**). A common way to predict the susceptibility of an alloy to form TCP phase is the calculation of the average electron-vacancy number ($\overline{N_v}$ number) according to the following equation given by Woodyatt et al. [10]:

$$\overline{N_v} = \sum_{i=1}^{n} m_i \left(N_v\right)_i$$

where: $\overline{N_v}$ = *average electron-vacancy number*

m_i = *atomic fraction of particular element i in the matrix*

$\left(N_v\right)_i$ = *individual electron-vacancy number of particular element i.*

Usually this method is applied to the nominal composition of an alloy, neglecting inhomogeneities caused by segregation during solidification. In the following this method will be applied to compositions measured by microprobe analysis along a dendrite arm.

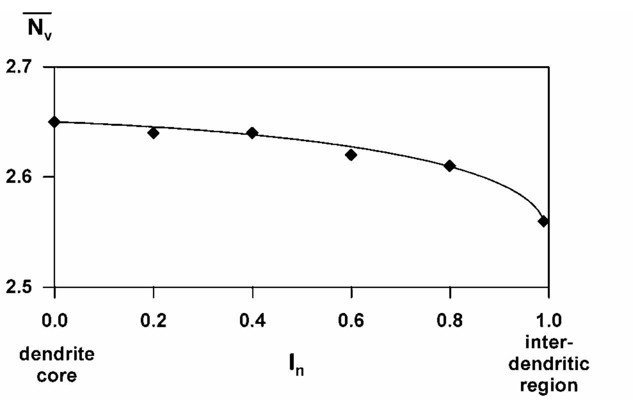

Figure 11: The average electron-vacancy number ($\overline{N_v}$ number) as a function of l_n, calculated based on the results shown in **Fig. 5**.

Using the microprobe results (**Fig. 5**) as input data for a $\overline{N_v}$ calculation leads to a $\overline{N_v}$ profile as shown in **Fig. 11**. The $\overline{N_v}$ value that approaches 2.65 in the dendrite core drops to 2.56 in the interdendritic region. Thus the dendrite core is particularly more prone to TCP phase formation than the interdendritic region.

Nucleation and growth of TCP phase occurred much more quickly in the coarser dendrite structure than in the finer dendrite structure. The concentration profile in **Fig. 5** has been measured for the coarser structure. The microprobe measurement technique is not accurate enough to allow for a direct comparison of the concentration profile in the two microstructures. It seems reasonable to assume that the homogenisation treatment results in a more homogeneous structure for the finer dendrites. This is because diffusional distances are smaller and diffusional flow is stronger (as it is driven by a stronger gradient due to the smaller diffusion distances).

Conclusions

In the alloy *ExAl7* investigated in the present work, TCP phase precipitated predominantly in the dendrite core. This correlates with a high refractory content in the core and consequently a high average electron-vacancy number.

TCP phase formation is stronger in the material with the coarser dendrite structure. This can be caused by less effective diffusional flow and homogenisation during heat treatment due to smaller concentration gradients and larger distances.

TCP phase precipitates were too small in length or volume fraction in the present case to affect either creep or fatigue strength. The fine and coarse dendrite structure produced in the present investigation represent the typical range in small aero-sengine turbine blades. Industrial gas turbines often feature much coarser dendrite structures. Much stronger effects are to be expected under such conditions.

Acknowledgements

A financial grant from the BMBF (German Ministry of Science and Education, Grant No. 03N2011C) is gratefully acknowledged. The authors also wish to express their special thanks to Doncaster Precision Castings Bochum GmbH for supporting this work by supply of materials and analysis data.

References

[1] B. B. Seth: Superalloys – The utility gas turbine perspective, in: T. M. Pollock et al. (eds.), *Superalloys 2000, Proc. 9th Int. Symp. on Superalloys, Seven Springs/PA* (The Minerals, Metals & Materials Society, Warrendale/PA), 2000, 3-16.

[2] R. Darolia, D. F. Lahrmann and R. D. Field: Formation of Topologically Closed Packed Phases in Nickel Base Single Crystal Superalloys, in: S. Reichmann et al. (eds.), *Superalloys 1988, Proc. 6th Int. Symp. on Superalloys, Seven Springs/PA* (The Minerals, Metals and Materials Society, Warrendale/PA, 1988), 255-264.

[3] G. L. Erickson: The development of the CMSX-11B and CMSX-11C alloys for industrial gas turbine applications, in: R. D. Kissinger et al. (eds.), *Superalloys 1996, Proc. 8th Int.*

Symp. on Superalloys, Seven Springs/PA (The Minerals, Metals & Materials Society, Warrendale/PA, 1996), 35-44.

[4] W. S. Walston, J. C. Schaeffer and W. H. Murphy: A new type of microstructural instability – SRZ, in R. D. Kissinger et al. (eds.), Superalloys 1996, *Proc. 8th Int. Symp. on Superalloys, Seven Springs/PA* (The Minerals, Metals & Materials Society, Warrendale/PA, 1996), 9-18.

[5] A. Volek, R. F. Singer, R. Bürgel, J. Großmann and Y. Wang: "Influence of TCP phase formation on creep rupture life of directionally solidified nickel-base superalloys," *to be published in Metallurgical and Materials Transactions A.*

[6] J. Großmann, J. Preuhs, W. Esser and R. F. Singer: Investment casting of high performance turbine blades by liquid metal cooling – a step forward towards industrial scale manufacturing, in A. Mitchell et al. (eds.), *Proc. 1999 Int. Symp. on Liquid Metal Processing and Casting*, Santa Fe/NM (American Vacuum Society, 1999), 21-24.

[7] A. Lohmüller, W. Eßer, J. Großmann, M. Hördler, J. Preuhs and R. F. Singer: Improved quality of investment castings by liquid metal cooling – the selection of cooling media, in T. M. Pollock et al. (eds.), Superalloys 2000, *Proc. 9th Int. Symp. on Superalloys, Seven Springs/PA* (The Minerals, Metals & Materials Society, Warrendale/PA, 2000), 181-188.

[8] T. J. Fitzgerald and R. F. Singer: "An analytical model for optimal directional solidification using liquid metal cooling," *Met. Trans. A*, 28 (1997) 6, 1189- 1199.

[9] R. Bürgel, J. Großmann, O. Lüsebrink, H. Mughrabi, F. Pyczak, R. F. Singer and A. Volek: Development of a new alloy for directional solidification of large industrial gas turbine blades, *submitted to Superalloys 2004, 10th Int. Symp. on Superalloys, Seven Springs/PA.*

[10] L. R. Woodyatt, C. T. Sims, H. J. Beattie, Prediction of sigma-type phase occurence from compositions in austenitic Superalloys, *T. Metall. Soc. AIME* 236 (1966) 519-527.